

Article

Fpr2^{-/-} Mice Developed Exacerbated Alcohol-Associated Liver Disease

Josiah E. Hardesty¹, Jeffrey B. Warner^{1,2}, Ying L. Song¹, Alison Floyd¹, Craig J. McClain^{1,2,3,4,5} , Dennis R. Warner¹ and Irina A. Kirpich^{1,2,4,5,6,*}

¹ Division of Gastroenterology, Hepatology, and Nutrition, Department of Medicine, University of Louisville, Louisville, KY 40202, USA

² Department of Pharmacology and Toxicology, University of Louisville, Louisville, KY 40202, USA

³ Robley Rex Veterans Medical Center, Louisville, KY 40202, USA

⁴ University of Louisville Alcohol Center, University of Louisville, Louisville, KY 40202, USA

⁵ University of Louisville Hepatobiology & Toxicology Center, University of Louisville, Louisville, KY 40202, USA

⁶ Department of Microbiology and Immunology, University of Louisville, Louisville, KY 40202, USA

* Correspondence: irina.kirpich@louisville.edu; Tel.: +1-(502)-852-7653

Simple Summary: Alcohol-associated liver disease (ALD) is a global healthcare problem, and the mechanisms of ALD development are not fully understood. In this study, we found that loss of formyl peptide receptor 2 (FPR2) worsened alcohol-induced injury and inflammation and altered liver regeneration. An exacerbation of ALD due to FPR2 gene knockout was associated with abnormal immune responses. This study demonstrated that FPR2 plays an important role in the pathogenesis of ALD.

Abstract: Alcohol-associated liver disease (ALD) is the most common chronic liver disease and carries a significant healthcare burden. ALD has no long-term treatment options aside from abstinence, and the mechanisms that contribute to its pathogenesis are not fully understood. This study aimed to investigate the role of formyl peptide receptor 2 (FPR2), a receptor for immunomodulatory signals, in the pathogenesis of ALD. WT and *Fpr2*^{-/-} mice were exposed to chronic-binge ethanol administration and subsequently assessed for liver injury, inflammation, and markers of regeneration. The differentiation capacity of liver macrophages and the oxidative burst activity of neutrophils were also examined. Compared to WT, *Fpr2*^{-/-} mice developed more severe liver injury and inflammation and had compromised liver regeneration in response to ethanol administration. *Fpr2*^{-/-} mice had fewer hepatic monocyte-derived restorative macrophages, and neutrophils isolated from *Fpr2*^{-/-} mice had diminished oxidative burst capacity. *Fpr2*^{-/-} MoMF differentiation was restored when co-cultured with WT neutrophils. Loss of FPR2 led to exacerbated liver damage via multiple mechanisms, including abnormal immune responses, indicating the crucial role of FPR2 in ALD pathogenesis.

Keywords: alcohol-associated liver disease; FPR2; restorative MoMFs



Citation: Hardesty, J.E.; Warner, J.B.; Song, Y.L.; Floyd, A.; McClain, C.J.; Warner, D.R.; Kirpich, I.A. *Fpr2*^{-/-} Mice Developed Exacerbated Alcohol-Associated Liver Disease. *Biology* **2023**, *12*, 639. <https://doi.org/10.3390/biology12050639>

Academic Editor: Paolo Parini

Received: 6 February 2023

Revised: 19 April 2023

Accepted: 21 April 2023

Published: 23 April 2023



Copyright: © 2023 by the authors. Licensee MDPI, Basel, Switzerland. This article is an open access article distributed under the terms and conditions of the Creative Commons Attribution (CC BY) license (<https://creativecommons.org/licenses/by/4.0/>).

1. Introduction

Alcohol-associated liver disease (ALD) is the most common chronic liver disease and a significant contributor to the global healthcare burden [1]. The spectrum of ALD ranges from liver steatosis to steatohepatitis, fibrosis, and cirrhosis. Worldwide, 500,000 annual cirrhosis deaths can be attributed to chronic alcohol consumption [2]. However, there is currently no effective FDA-approved therapy to halt or reverse ALD in humans. The pathogenesis of ALD is complex, with multiple molecules, signaling pathways, and cell types involved. Several mechanisms have been identified in ALD development and progression, including increased intestinal permeability and gut-derived endotoxemia [3], immune system dysfunction [4], hepatocellular death [5], and inflammation [6], among

others. Impaired liver regeneration due to a loss of hepatocyte proliferation following alcohol-induced damage has also been identified as a contributing factor to the pathogenesis of ALD [7,8]. The elucidation of new molecules and signaling pathways contributing to ethanol-induced liver injury and altered regeneration may lead to the development of novel therapeutics for this disease.

Formyl peptide receptor 2 (FPR2) is a G-protein-coupled receptor highly expressed in multiple immune cells such as neutrophils, macrophages, monocytes, and monocyte-derived macrophages [MoMFs] [9,10]. FPR2 interacts with various ligands, which elicit a plethora of effects [10]. One such ligand is bacteria-derived N-Formyl methionyl-leucyl-phenylalanine, which stimulates neutrophil chemotaxis in vitro [11]. FPR2 ligands that originate from the host, e.g., Annexin A1, have been shown to increase IL-10 production in monocytes [12]. Resolvin D1 is another host-derived FPR2 ligand that can promote M2 polarization of hepatic macrophages and increase efferocytosis capacity [13]. It has been shown that the loss of FPR2 can exacerbate the pathology of several diseases [13–16]. Previous studies demonstrated that *Fpr2*^{−/−} mice developed exacerbated liver injury and inflammation in animal models of sepsis [17] and increased mortality after bacterial infections [14]. In a diet-induced, non-alcohol-associated fatty liver disease model, *Fpr2*^{−/−} mice also developed exacerbated liver injury and inflammation [15]. However, the role of FPR2 in ALD pathogenesis has not been investigated. In the current study, we aimed to examine whether *Fpr2* genetic deletion can exacerbate ethanol (EtOH)-induced liver injury in an animal model of acute-on-chronic EtOH administration and identify the contributing mechanisms.

2. Materials and Methods

2.1. Animal Studies

Fpr2^{−/−} mice on a C57BL/6J background were generated by Dr. Mauro Perretti [18] and obtained from Dr. Asma Nusrat (University of Michigan). Mice were housed in a temperature-controlled room (23.9 °C) with a 12 h light-dark cycle. Experimental *Fpr2*^{−/−} mice were bred in-house and genotyped as detailed in [18]. qRT-PCR analysis confirmed that *Fpr2*^{−/−} mice did not express the *Fpr2* transcript (Figure S1). Female *Fpr2*^{−/−} and WT littermates aged 8–10 weeks were administered Lieber-DeCarli EtOH-containing or isocaloric control diets (Products F1258SP and F1259SP, respectively; BioServ, Flemington, NJ, USA) as follows: 1% (v/v) and 2% (v/v) for two days each, 5% (v/v) for 2 weeks, and then 4% (v/v) for one week. On the final day, the EtOH group received a binge of EtOH (5 g/kg) delivered by oral gavage. Animals were euthanized 9 h after the EtOH binge. There were four experimental groups in this study: WT PF (*n* = 8), WT + EtOH (*n* = 10), *Fpr2*^{−/−} PF (*n* = 5), and *Fpr2*^{−/−} + EtOH (*n* = 8). All animal experiments were conducted in accordance with the guidelines set forth by the University of Louisville Institutional Animal Care and Use Committee under an approved protocol (number 18418 to IAK).

2.2. Measurement of Plasma ALT Activity and Endotoxin Levels

Plasma ALT activity was determined using the Infinity™ ALT Reagent (Thermo Fisher Scientific, Waltham, MA, USA). Plasma endotoxin levels were measured with the Chromo LAL kit from Associates of Cape Cod, Inc. (East Falmouth, MA, USA) according to the manufacturer's instructions.

2.3. Immunoassay of TNFα in Liver Tissue

Liver samples (~100 mg) were homogenized in modified RIPA buffer (50 mM Tris, 150 mM NaCl, 0.1% Triton X-100, 0.5% sodium deoxycholate, 0.1% SDS) supplemented with protease and phosphatase inhibitors (Halt™, Thermo Fisher Scientific, Waltham, MA, USA) in tubes filled with 0.5 mm glass beads (BioSpec, Bartlesville, OK, USA). Following centrifugation at 16,000× *g*, supernatants were collected, and protein concentrations were determined by the BCA method. A total of 600 µg of liver protein was analyzed on the V-PLEX immunoassay platform for TNFα. The data were collected on the MESO Sector S

600 instrument and then analyzed using Discovery Workbench v. 4.0 software (all from MesoScale Discovery, Rockville, MD, USA).

2.4. Histopathological and Immunohistochemical Analysis of Liver Tissue

Formalin-fixed, paraffin-embedded liver samples were sectioned (5 μm), stained with either H & E, chloroacetate esterase (CAE, Sigma Aldrich, St. Louis, MO, USA), TUNEL (ApopTag, EMD Millipore Sigma, St. Louis, MO, USA), or immunostained for CD163 (Abcam, Cambridge, UK) and PCNA (Cell Signaling Technology, Danvers, MA, USA). Quantification was performed by counting CAE-positive, TUNEL-positive, or PCNA-positive cells in a random series of ten digital images per section (200 \times field). The number of positive cells was summed and averaged to obtain an estimate for each mouse ($n = 5\text{--}10$ mice/group). The cryopreserved liver sections were cut into 5 μm sections and then stained with Oil Red O and counterstained with hematoxylin. The percentage of Oil Red O-positive or CD163-positive area was calculated with Image J. For each mouse liver section, ten randomized images were used, following a previously described method [19].

2.5. Liver Triglycerides Extraction and Measurement

Liver lipid extracts were measured as previously described [20] using the InfinityTM Triglyceride Liquid Stable Reagent (Thermo Fisher Scientific, Waltham, MA, USA).

2.6. RNA Isolation and Real-Time Quantitative Reverse Transcription PCR (RT-qPCR)

Total RNA from the liver was isolated with Trizol reagent (Thermo Fisher Scientific, Waltham, MA, USA) as described by the manufacturer, and any contaminating genomic DNA was removed by digestion with DNase I (Thermo Fisher Scientific, Waltham, MA, USA). cDNA was synthesized with qScript cDNA Supermix (Quanta Biosciences, Beverly, MA, USA) from 1 μg of RNA. RT-qPCR assays were performed with PerfeCTa SYBR Green Fast Mix (Quanta Biosciences) on the BioRad CFX384 instrument (Bio-Rad, Hercules, CA, USA). The data were analyzed by the $\Delta\Delta\text{Ct}$ method [21]. Primers for RT-qPCR analysis are listed in Supporting Table S2.

2.7. Flow Cytometry Analysis of Neutrophils

Neutrophils were isolated from whole blood acquired from naïve WT and *Fpr2*^{-/-} mice ($n = 3$ per genotype) by immunomagnetic negative selection with the EasyStep Mouse Neutrophil Enrichment Kit (StemCell, Vancouver, CA, USA). Preparations with >95% neutrophils (Ly6G⁺/CD11b⁺) were used for assays. Neutrophils were incubated with or without lipopolysaccharide (LPS) (100 ng/mL) for 30 min, followed by assessment of oxidative burst (i.e., superoxide via MitoSOX staining). Neutrophils were analyzed by flow cytometry using a BD FACS Canto II flow cytometer (BD Biosciences, Franklin Lakes, NJ, USA), and data were analyzed via FlowJo software (Ashland, OR, USA).

2.8. Measurement of Liver MPO Activity and H₂O₂ Levels

Liver lysates (200 μg of protein) were used to detect MPO activity and H₂O₂ levels using the myeloperoxidase chlorination activity assay (Cell Biolabs, San Diego, CA, USA) and a peroxide assay kit (Sigma-Aldrich, St. Louis, MO, USA), respectively.

2.9. Flow Cytometry Analysis

BMDMs and hepatic non-parenchymal cells were isolated from WT and *Fpr2*^{-/-} mice ($n = 3$ per genotype) as previously described [22]. Cells were then immunostained with PE-F4/80, FITC-Ly6C, and PerCy5.5-Cd11b (Invitrogen, Waltham, MA, USA) to identify the monocyte (F4/80^{lo}, Ly6C^{hi}, Cd11b⁺) and MoMF populations (F4/80^{hi}, Ly6C^{lo}, Cd11b⁺) by flow cytometry.

2.10. BMDM and Neutrophil Co-Culture Experiment

Bone marrow was isolated from WT and *Fpr2*^{-/-} ($n = 3$ per genotype) as described in Section 2.9. Neutrophils were isolated from the bone marrow by positive selection using Ly6G antibodies and MACS LS columns (Miltenyi, Gaithersburg, MD, USA). WT and *Fpr2*^{-/-} bone marrow cells and neutrophils were then cross-cultured at a 5:1 ratio (500,000 bone marrow to 100,000 neutrophils) [23,24] in BMDM differentiation media \pm catalase (100 nM). The culture medium was changed after 48 h to remove dead and non-adherent cells. The culture was continued in L929, which contained media, for an additional 5 days. Cells were then immunostained and analyzed by flow cytometry as described in Section 2.9.

2.11. Statistical Analysis

Data were analyzed using an unpaired Student's *t*-test (two groups) and a one-way ANOVA (more than two groups), followed by the appropriate post hoc analyses to determine significant differences between experimental groups. Data are presented as the mean \pm standard error of the mean (SEM). A $p < 0.05$ was considered statistically significant.

3. Results

3.1. *Fpr2*^{-/-} Mice Developed Exacerbated Acute-on-Chronic Alcohol-Induced Liver Injury and Inflammation

WT and *Fpr2*^{-/-} mice were fed either an EtOH or control isocaloric diet (EtOH-fed or pair-fed [PF], respectively) for 4 weeks, followed by a single EtOH binge at the end of the feeding protocol. Both WT and *Fpr2*^{-/-} mice tolerated the experimental protocol, and no mortality was observed. Food consumption was similar for all experimental groups (Table S1). The effects of genotype on metabolic parameters in response to EtOH administration are presented in Table S1. Body weight increase was significantly higher in EtOH-fed mice relative to PF for both WT and *Fpr2*^{-/-} mice. The liver-to-body weight ratio was reduced in *Fpr2*^{-/-} mice fed EtOH compared to WT EtOH mice, while the white adipose tissue-to-body weight ratio was only significantly higher in *Fpr2*^{-/-} EtOH mice relative to *Fpr2*^{-/-} PF mice.

Fpr2 deficiency significantly exacerbated acute-on-chronic alcohol-induced liver injury in EtOH-fed *Fpr2*^{-/-} mice as compared to WT EtOH mice, as determined by elevated plasma ALT activity (Figure 1A). Liver steatosis was modestly increased in both WT and *Fpr2*^{-/-} EtOH-fed mice as determined by liver hematoxylin and eosin (H & E) staining (Figure 1B), liver triglyceride measurement (Figure 1C), and Oil Red O staining (Figure 1D,E) and was comparable between genotypes. The number of TUNEL-positive cells was significantly increased in *Fpr2*^{-/-} EtOH-fed mice but not in WT EtOH-fed mice compared to PF mice, indicating a higher level of EtOH-induced hepatocellular death in the *Fpr2*^{-/-} mice than in the WT mice (Figure 1F,G). Further, EtOH administration resulted in increased endotoxemia (Figure 1H) in both genotypes and was significantly higher in EtOH-fed *Fpr2*^{-/-} vs. WT mice. Compared to PF mice, hepatic TNF α levels, a marker of inflammation, were significantly elevated in *Fpr2*^{-/-} mice fed EtOH but not in WT mice fed EtOH (Figure 1I). Collectively, our data demonstrated that loss of *Fpr2* resulted in more severe EtOH-induced liver injury and inflammation.

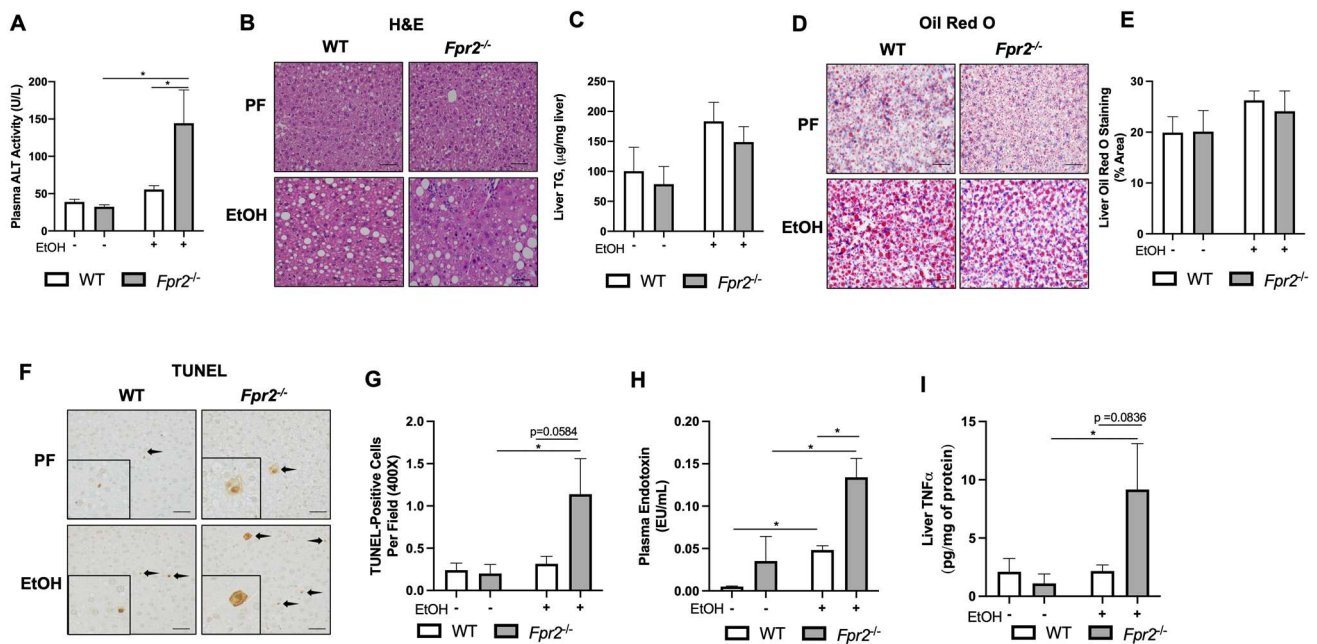


Figure 1. *Fpr2*^{-/-} mice developed exacerbated acute-on-chronic alcohol-induced liver injury and inflammation. (A) Plasma ALT activity. (B) Representative H & E-stained liver sections were imaged at 200×. The scale bar is 100 µm. (C) Liver triglyceride measurement. (D,E) Representative Oil Red O-stained liver sections were imaged at 400× and quantified via Image J to quantify the percent area of Oil Red-O staining. (F) Representative TUNEL-stained liver sections were imaged at 400×. The scale bar is 100 µm. (G) Quantification of TUNEL-positive cells is from the average of 10 randomized fields per mouse. (H) Plasma endotoxin levels. (I) Hepatic TNFα levels. Data are presented as mean ± SEM and were statistically compared by a one-way ANOVA with Sidak's multi-comparison test for parametric data and a Kruskal–Wallis test with Dunn's multiple comparisons test for non-parametric data; * *p* < 0.05.

3.2. Effect of *Fpr2* Genetic Ablation on Markers of Liver Regeneration in Response to EtOH

Compromised liver regeneration is a hallmark of severe ALD [7]. Therefore, we investigated the effect of *Fpr2* deficiency on this process. Immunohistochemical staining revealed no quantitative differences in PCNA-positive hepatocytes among experimental groups (Figure 2A,B). RT-qPCR analysis showed that both WT and *Fpr2*^{-/-} mice had EtOH-induced *Pcna* and *Ki67* gene expression (Figure 2C,D). Of note, the levels of these markers were significantly lower in *Fpr2*^{-/-} vs. WT EtOH-fed animals, suggesting that *Fpr2* genetic ablation may compromise liver regeneration in response to an EtOH insult. There were no statistically significant differences between WT PF and *Fpr2*^{-/-} PF mice in *Pcna* (likely due to the high intragroup variability in the WT PF group) as well as *Ki67* gene expression.

Multiple cell types participate in liver regeneration, including restorative MoMFs [25]. In response to EtOH administration, *Fpr2* genetic deletion resulted in reduced numbers of hepatic MoMFs in *Fpr2*^{-/-} EtOH as compared to WT EtOH-fed mice. This was shown by decreased hepatic staining (Figure 3A,B) and expression of *Cd163* (Figure 3C), *Mertk* (Figure 3D), and *Mrc1* (Figure 3E), well-recognized MoMFs markers [25–27]. Flow cytometry analysis further confirmed that *Fpr2*^{-/-} mice had intrinsically lower levels of hepatic MoMFs as compared to WT mice (Figure S2).

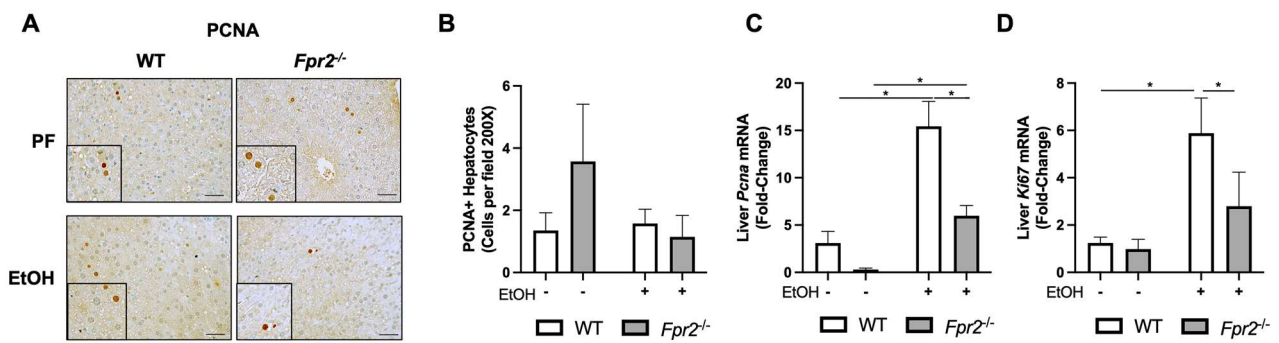


Figure 2. Effect of *Fpr2* genetic ablation on markers of liver regeneration in response to EtOH. (A,B) Representative PCNA-immunostained liver sections were imaged at 400× and quantified. The scale bar is 100 μm. PCNA-positive hepatocytes were manually counted and averaged for 10 randomized fields for each mouse liver section. (C,D) Hepatic *Pcna* and *Ki67* gene expression. Data are presented as mean ± SEM and were statistically compared by a one-way ANOVA with Sidak’s multi-comparisons test for parametric data and a Kruskal–Wallis test with Dunn’s multiple comparison tests for non-parametric data; * *p* < 0.05.

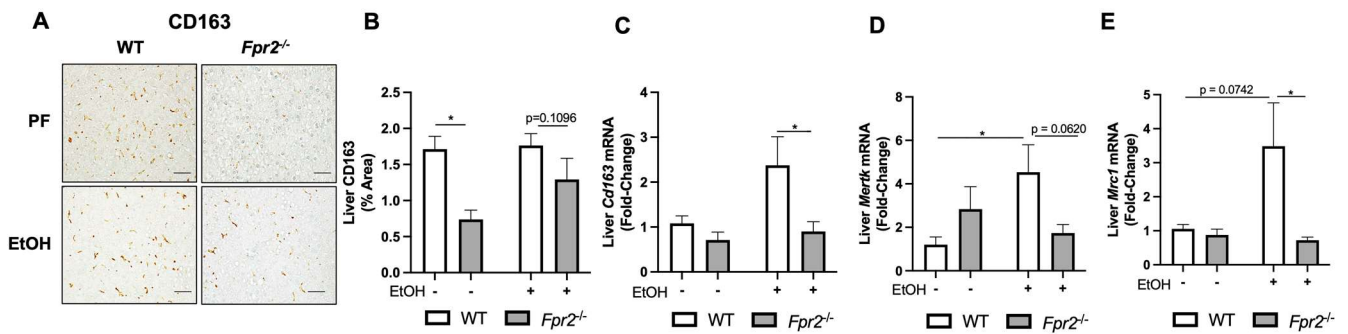


Figure 3. *Fpr2* deletion resulted in reduced hepatic restorative MoMFs in vivo. (A,B) Representative CD163-immunostained liver sections were imaged at 400× and quantified. The scale bar is 100 μm. Images from 10 randomized fields per mouse liver section were analyzed in Image J to quantify the average percent area of CD163. (C) Hepatic *Cd163* gene expression. (D,E) Hepatic gene expression of *Mertk* and *Mrc1*. Data are presented as mean ± SEM and were statistically compared by a one-way ANOVA with Sidak’s multi-comparisons test for parametric data and a Kruskal–Wallis test with Dunn’s multiple comparisons test for non-parametric data; * *p* < 0.05.

Next, we examined the role of *Fpr2* in MoMF differentiation in vitro using bone marrow-derived macrophages (BMDMs) isolated from naïve WT and *Fpr2*^{-/-} mice. A standard macrophage differentiation protocol [28] was followed by flow cytometry analysis to measure the number of monocytes and MoMFs (Figure 4A). We found that the monocyte population was significantly higher, while the MoMF population was significantly lower in *Fpr2*^{-/-} relative to WT mice-derived cells (Figure 4B–D). This suggests that loss of *Fpr2* expression compromises monocyte-to-macrophage differentiation potential.

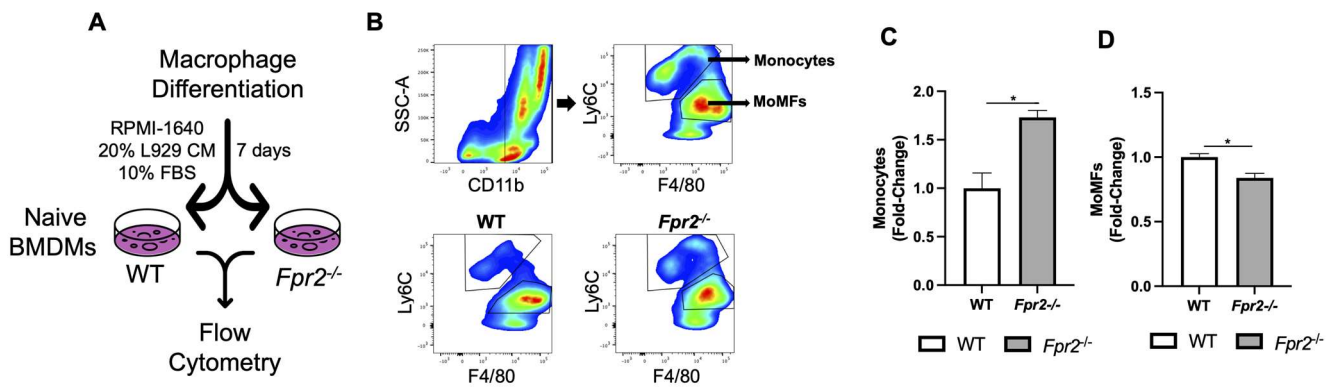


Figure 4. *Fpr2*^{-/-} bone marrow progenitors had reduced MoMF differentiation potential in vitro. (A) Model of BMDM differentiation. (B) Gating strategy for flow cytometry analysis, and representative flow cytometry plots for WT and *Fpr2*^{-/-} monocytes and MoMFs. (C,D) Quantification of monocytes and MoMFs for WT and *Fpr2*^{-/-} cells. The data for this figure are an average of three independent experiments using individual mice of each genotype. Data are presented as mean ± SEM and were statistically compared by an unpaired Student's *t*-test; * *p* < 0.05.

3.3. Liver Damage in EtOH-fed *Fpr2*^{-/-} Mice was Associated with Alterations in Neutrophil Oxidative Burst

It has been recently shown that hepatic neutrophils may promote monocyte differentiation to MoMFs via the release of oxidative species (e.g., H₂O₂ and O₂⁻) [29]. First, we examined the effects of genotype and EtOH administration on hepatic neutrophil infiltration. There was a trending increase in hepatic neutrophils in response to EtOH in both genotypes (although not significant), which was higher in *Fpr2*^{-/-} mice (Figure 5A,B). Another marker of neutrophils, hepatic MPO activity, was significantly elevated by EtOH in *Fpr2*^{-/-} but not in WT mice (Figure 5C). Next, hepatic H₂O₂ levels were examined, which were increased in EtOH-fed mice in both genotypes, reaching statistical significance, however, only in WT animals (Figure 5D). Importantly, there was a significant decrease in hepatic H₂O₂ levels in EtOH-fed *Fpr2*^{-/-} vs. WT mice. Since neutrophil oxidative burst is compromised in severe ALD [30] and can positively regulate MoMF differentiation [29], we further investigated the effects of *Fpr2* ablation on neutrophil oxidative burst in vitro. Both basal and LPS-stimulated oxidative bursts, as measured by superoxide production, significantly decreased in *Fpr2*^{-/-} neutrophils (Figure 5E,F). These findings may indicate that neutrophil-derived factors contributing to MoMF differentiation are altered with *Fpr2* ablation.

3.4. *Fpr2*^{-/-} Bone Marrow Cells can Differentiate into MoMFs when Co-Cultured with WT Neutrophils

Recently, it has been demonstrated that neutrophils can promote MoMF differentiation via an H₂O₂-dependent mechanism [29]. To test if a reduction in H₂O₂ production by *Fpr2*^{-/-} neutrophils contributed to compromised MoMF differentiation, we co-cultured neutrophils and bone marrow cells isolated from WT and *Fpr2*^{-/-} mice (Figure 6A). When neutrophils and BM cells from *Fpr2*^{-/-} mice were cultured, there were reduced numbers of MoMFs as compared to when cells from WT mice were cultured (Figure 6B). Co-culture of WT BM cells with *Fpr2*^{-/-} neutrophils resulted in a similar reduction in MoMFs. Next, when WT neutrophils and *Fpr2*^{-/-} BM cells were co-cultured, there was a rescue in the number of MoMFs equal to that observed when WT neutrophils and BM cells were co-cultured. There was a corresponding increase or decrease in monocytes observed for the various treatments, as seen in Figure 6C. Lastly, these effects appear to be due to H₂O₂ since catalase-treated cells had a reduction in MoMFs with a concomitant increase in monocytes, as previously reported [29,31].

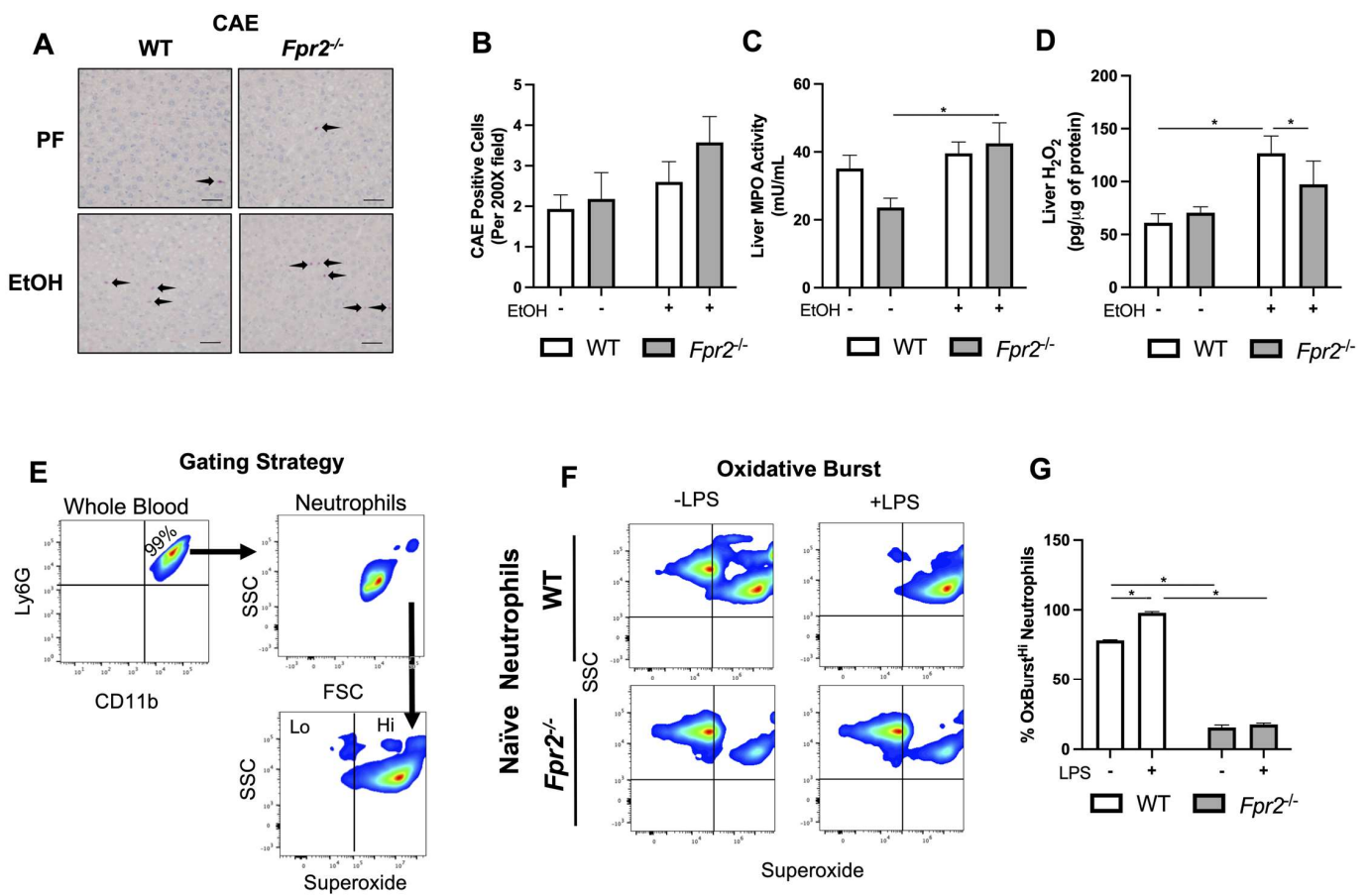


Figure 5. Liver damage in EtOH-fed *Fpr2*^{-/-} mice was associated with compromised neutrophil oxidative burst. (A) Representative CAE-stained liver sections were imaged at 400×. Scale bar is 100 μm (B) Quantification of CAE-positive cells from 10 randomized fields of view were averaged per mouse. (C) Hepatic MPO activity. (D) Hepatic H₂O₂ levels. (E) Flow cytometry gating strategy for assessment of oxidative burst in neutrophils. (F) Representative flow cytometry plots of WT and *Fpr2*^{-/-} neutrophil assessment for oxidative burst. (G) Quantification of high oxidative burst (increased superoxide) neutrophil populations between genotypes. Data for (E–G) are an average of three independent experiments using individual mice of each genotype. Data are presented as mean ± SEM and were statistically compared by a one-way ANOVA with Sidak’s multi-comparisons test for parametric data and a Kruskal–Wallis test with Dunn’s multiple comparisons test for non-parametric data; * *p* < 0.05.

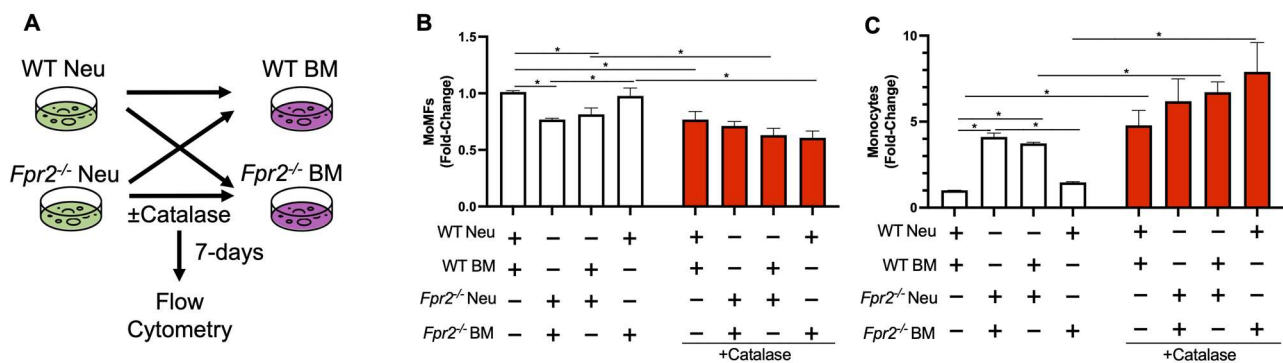


Figure 6. *Fpr2*^{-/-} bone marrow cells can differentiate into MoMFs when co-cultured with WT neutrophils. (A) Schematic of WT and *Fpr2*^{-/-} neutrophils and bone marrow cells being co-cultured and MoMF differentiation being evaluated by flow cytometry analysis. Changes in (B) MoMFs and (C) monocytes under various co-culture conditions. The data for this figure are an average of three independent experiments using individual mice of each genotype. Data are presented as mean ± SEM and were statistically compared by a one-way ANOVA with Sidak's multi-comparisons test for parametric data and a Kruskal–Wallis test, * *p* < 0.05.

4. Discussion

In the present study, we investigated the effects of the genetic deletion of *Fpr2* in an experimental animal model of ALD. FPR2 is a G-protein-coupled receptor that is highly expressed in multiple immune cell types [32,33] and interacts with numerous ligands to regulate distinct signaling cascades and processes, including immune responses [10,34]. We found that loss of *Fpr2* exacerbated experimental EtOH-induced liver injury and inflammation, which was associated with compromised liver regeneration. Our findings are consistent with recent studies demonstrating worsened pathology in *Fpr2*^{-/-} mice in animal models of various diseases. For example, compared to WT, female *Fpr2*^{-/-} mice in a dietary model of non-alcohol-associated fatty liver disease had enhanced hepatocellular death and inflammation, as shown by elevated hepatic TNF α levels [15]. In a separate study, LPS-challenged *Fpr2*^{-/-} mice had increased liver injury, elevated levels of hepatic TNF α and immune cell infiltration, and reduced liver regeneration [16]. Our observations, paired with previously reported studies, demonstrate a shared phenotype of exacerbated liver injury, inflammation, and moderately compromised regeneration in *Fpr2*^{-/-} mice following distinct insults such as diet, LPS, or alcohol.

Compromised liver regeneration is frequently observed in patients with ALD [7,8,35]. However, underlying mechanisms are still under-investigated and not fully understood. It has been shown that the depletion of hepatic macrophages results in compromised liver regeneration in EtOH-fed mice [36]. Recently, restorative MoMFs have been identified as an important cell population in the coordination of liver regeneration via the resolution of inflammation and the release of pro-regenerative growth factors [25]. In our animal model, we observed alterations in markers of liver regeneration in response to EtOH in *Fpr2*^{-/-} vs. WT mice. We also found reduced hepatic MoMF markers in *Fpr2*^{-/-} mice in vivo and reduced MoMF differentiation capacity in vitro in BMDMs from *Fpr2*^{-/-} animals. This suggests that FPR2 may play a role in MoMF differentiation via interaction with one of its ligands. Previously, FPR2 activation by a synthetic FPR2 agonist was shown to increase the number of pro-resolution macrophages in an animal model of myocardial infarction [37]. Since many ligands interact with FPR2, future studies are warranted to determine which FPR2 ligands may promote monocyte-to-MoMF differentiation. Other MoMF factors have also been described, such as IL-10 [38] and SLPI [27]. For example, treatment with blocking antibodies to IL-10 delayed the monocyte-to-MoMF transition in an animal model of liver injury [38]. Previously, *Fpr2*^{-/-} mice have been shown to produce less IL-10 [12], suggesting that loss of *Fpr2* may impact MoMF differentiation via reduced IL-10 production.

Monocytes can differentiate into restorative MoMFs by neutrophil-derived signals as well, such as reactive oxygen species (ROS), that in turn stimulate hepatocyte proliferation [29]. In our study, we observed increased hepatic neutrophil infiltration but compromised function, including oxidative burst, associated with the depletion of neutrophil-derived ROS (e.g., H₂O₂ and superoxide) in *Fpr2*^{-/-} mice. Likely, a loss of neutrophil ROS contributed to the reduced number of MoMFs observed in *Fpr2*^{-/-} mice. Indeed, we found that WT neutrophils could restore *Fpr2*^{-/-} MoMF differentiation, which was attenuated by catalase. Of note, monocytes can also produce H₂O₂ upon treatment with M-CSF (present in L929 media), which can contribute to their differentiation [31], thus explaining why catalase treatment did not fully ablate MoMF differentiation in the present study. The role of FPR2 in neutrophil oxidative burst was also previously demonstrated in in vitro studies. This shows that FPR2 activation in HL-60 cells (a neutrophil-like cell line) by the FPR2 ligand BMS-986235 stimulated an oxidative burst, but this was completely ablated with the loss of FPR2 [37]. Phosphoregulation of NADPH oxidase subunits was recently identified as one of the mechanisms by which FPR2 may mediate an oxidative burst [39]. Our findings are relevant to human ALD since AH patients have impaired neutrophil oxidative burst [30], which may contribute to altered liver regeneration. Future studies will aim to investigate the neutrophil and MoMF crosstalk in pre-clinical and clinical ALD and determine if FPR2 agonists have therapeutic potential.

The current study is novel and relevant to the field of ALD, but it has some potential limitations. In this study, only female mice were examined, taking into account that females develop exacerbated ALD when compared to males [40,41]. However, sex-specific differences are important considerations for future studies. The use of immune cells from the bone marrow and blood for in vitro studies might be another limitation of this study. However, neutrophils and monocytes originate from the bone marrow and infiltrate the liver upon chemokine signaling in response to liver injury [42], suggesting that the effects observed in these studies may mimic what occurs in the liver. Lastly, since *Fpr2* is also expressed in hepatocytes [33], future studies are warranted to examine its hepatocyte cell-specific effects in ALD.

5. Conclusions

Fpr2^{-/-} mice developed exacerbated alcohol-induced liver injury and inflammation in an experimental model of ALD. Additionally, the limited liver regeneration observed in *Fpr2*^{-/-} mice in response to EtOH is due to mechanisms involved in immune cell dysregulation, such as a reduced number of MoMFs, which is likely a result of impaired differentiation due to reduced neutrophil-derived H₂O₂. This study suggests that FPR2 may play a pivotal role in the differentiation of monocytes into MoMFs in ALD. The observed phenotype in *Fpr2*^{-/-} mice is reflective of what occurs in human AH, providing a rationale for evaluating FPR2 as a therapeutic target in human ALD.

Supplementary Materials: The following supporting information can be downloaded at: <https://www.mdpi.com/article/10.3390/biology12050639/s1>, Figure S1: Liver *Fpr2* mRNA expression; Figure S2: Liver MoMFs; Table S1: Metabolic characteristics of experimental mice. Table S2: qPCR Primers.

Author Contributions: Conceptualization, I.A.K., D.R.W. and J.E.H.; methodology, J.E.H., J.B.W., D.R.W. and Y.L.S.; software, J.E.H.; validation, J.E.H.; formal analysis, I.A.K., D.R.W., J.E.H., A.F. and J.B.W.; investigation, I.A.K. and J.E.H.; resources, I.A.K. and C.J.M.; data curation, J.E.H.; writing—original draft preparation, J.E.H. and I.A.K.; writing—review and editing, J.E.H., I.A.K., D.R.W., J.B.W. and C.J.M.; visualization, J.E.H. and J.B.W.; supervision, I.A.K.; project administration, I.A.K.; funding acquisition, I.A.K., C.J.M., J.B.W. and J.E.H. All authors have read and agreed to the published version of the manuscript.

Funding: This research was funded by the following grants: National Institutes of Health grants R01AA028905 (I.A.K.), F32AA027950 (J.E.H.), K99AA030627 (J.E.H.), F31AA028423 (J.B.W.), U01AA026934 (C.J.M.), U01AA026926 (C.J.M.), U01AA026980 (C.J.M.), R01AA023681 (C.J.M.), and the Intramural Programs of the National Institute on Alcohol Abuse and Alcoholism. This work was also supported by an Institutional Development Award (IDeA) from the National Institute of General Medical Sciences of the National Institutes of Health under grant number P20GM113226 (C.J.M.) and the National Institute on Alcohol Abuse and Alcoholism of the National Institutes of Health under award number P50AA024337 (C.J.M.). The content is solely the responsibility of the authors and does not necessarily represent the official views of the National Institutes of Health.

Institutional Review Board Statement: All animal experiments were conducted in accordance with the guidelines set forth by the University of Louisville Institutional Animal Care and Use Committee under an approved protocol (number 18418 to IAK).

Informed Consent Statement: Not applicable.

Data Availability Statement: The data presented in this study are available within this article and supplementary material.

Conflicts of Interest: The authors declare no conflict of interest.

References

1. Seitz, H.K.; Bataller, R.; Cortez-Pinto, H.; Gao, B.; Gual, A.; Lackner, C.; Mathurin, P.; Mueller, S.; Szabo, G.; Tsukamoto, H. Alcoholic liver disease. *Nat. Rev. Dis. Prim.* **2018**, *4*, 16. [[CrossRef](#)]
2. Asrani, S.K.; Devarbhavi, H.; Eaton, J.; Kamath, P.S. Burden of liver diseases in the world. *J. Hepatol.* **2019**, *70*, 151–171. [[CrossRef](#)]
3. Rao, R. Endotoxemia and gut barrier dysfunction in alcoholic liver disease. *Hepatology* **2009**, *50*, 638–644. [[CrossRef](#)] [[PubMed](#)]
4. Nagy, L.E. The Role of Innate Immunity in Alcoholic Liver Disease. *Alcohol Res.* **2015**, *37*, 237–250.
5. Wang, S.; Pacher, P.; De Lisle, R.C.; Huang, H.; Ding, W.X. A Mechanistic Review of Cell Death in Alcohol-Induced Liver Injury. *Alcohol Clin. Exp. Res.* **2016**, *40*, 1215–1223. [[CrossRef](#)]
6. Wang, H.J.; Gao, B.; Zakhari, S.; Nagy, L.E. Inflammation in alcoholic liver disease. *Annu. Rev. Nutr.* **2012**, *32*, 343–368. [[CrossRef](#)]
7. Lv, Y.; So, K.F.; Xiao, J. Liver regeneration and alcoholic liver disease. *Ann. Transl. Med.* **2020**, *8*, 567. [[CrossRef](#)] [[PubMed](#)]
8. Horiguchi, N.; Ishac, E.J.; Gao, B. Liver regeneration is suppressed in alcoholic cirrhosis: Correlation with decreased STAT3 activation. *Alcohol* **2007**, *41*, 271–280. [[CrossRef](#)]
9. Uhlen, M.; Oksvold, P.; Fagerberg, L.; Lundberg, E.; Jonasson, K.; Forsberg, M.; Zwahlen, M.; Kampf, C.; Wester, K.; Hober, S.; et al. Towards a knowledge-based Human Protein Atlas. *Nat. Biotechnol.* **2010**, *28*, 1248–1250. [[CrossRef](#)] [[PubMed](#)]
10. Weiß, E.; Kretschmer, D. Formyl-Peptide Receptors in Infection, Inflammation, and Cancer. *Trends Immunol.* **2018**, *39*, 815–829. [[CrossRef](#)] [[PubMed](#)]
11. Hartt, J.K.; Barish, G.; Murphy, P.M.; Gao, J.L. N-formylpeptides induce two distinct concentration optima for mouse neutrophil chemotaxis by differential interaction with two N-formylpeptide receptor (FPR) subtypes. Molecular characterization of FPR2, a second mouse neutrophil FPR. *J. Exp. Med.* **1999**, *190*, 741–747. [[CrossRef](#)] [[PubMed](#)]
12. Cooray, S.N.; Gobbetti, T.; Montero-Melendez, T.; McArthur, S.; Thompson, D.; Clark, A.J.; Flower, R.J.; Perretti, M. Ligand-specific conformational change of the G-protein-coupled receptor ALX/FPR2 determines proresolving functional responses. *Proc. Natl. Acad. Sci. USA* **2013**, *110*, 18232–18237. [[CrossRef](#)] [[PubMed](#)]
13. Kang, J.W.; Lee, S.M. Resolvin D1 protects the liver from ischemia/reperfusion injury by enhancing M2 macrophage polarization and efferocytosis. *Biochim. Biophys. Acta* **2016**, *1861*, 1025–1035. [[CrossRef](#)] [[PubMed](#)]
14. Oldekamp, S.; Pscheidl, S.; Kress, E.; Soehnlein, O.; Jansen, S.; Pufe, T.; Wang, J.M.; Tauber, S.C.; Brandenburg, L.O. Lack of formyl peptide receptor 1 and 2 leads to more severe inflammation and higher mortality in mice with of pneumococcal meningitis. *Immunology* **2014**, *143*, 447–461. [[CrossRef](#)]
15. Lee, C.; Kim, J.; Han, J.; Oh, D.; Kim, M.; Jeong, H.; Kim, T.J.; Kim, S.W.; Kim, J.N.; Seo, Y.S.; et al. Formyl peptide receptor 2 determines sex-specific differences in the progression of nonalcoholic fatty liver disease and steatohepatitis. *Nat. Commun.* **2022**, *13*, 578. [[CrossRef](#)]
16. Giebeler, A.; Streetz, K.L.; Soehnlein, O.; Neumann, U.; Wang, J.M.; Brandenburg, L.O. Deficiency of formyl peptide receptor 1 and 2 is associated with increased inflammation and enhanced liver injury after LPS-stimulation. *PLoS ONE* **2014**, *9*, e100522. [[CrossRef](#)] [[PubMed](#)]
17. Gobbetti, T.; Coldewey, S.M.; Chen, J.; McArthur, S.; le Faouder, P.; Cenac, N.; Flower, R.J.; Thiemermann, C.; Perretti, M. Nonredundant protective properties of FPR2/ALX in polymicrobial murine sepsis. *Proc. Natl. Acad. Sci. USA* **2014**, *111*, 18685–18690. [[CrossRef](#)]

18. Dufton, N.; Hannon, R.; Brancaleone, V.; Dalli, J.; Patel, H.B.; Gray, M.; D'Acquisto, F.; Buckingham, J.C.; Perretti, M.; Flower, R.J. Anti-inflammatory role of the murine formyl-peptide receptor 2: Ligand-specific effects on leukocyte responses and experimental inflammation. *J. Immunol.* **2010**, *184*, 2611–2619. [[CrossRef](#)]
19. Warner, D.R.; Warner, J.B.; Hardesty, J.E.; Song, Y.L.; Chen, C.Y.; Chen, Z.; Kang, J.X.; McClain, C.J.; Kirpich, I.A. Beneficial effects of an endogenous enrichment in n3-PUFAs on Wnt signaling are associated with attenuation of alcohol-mediated liver disease in mice. *FASEB J.* **2021**, *35*, e21377. [[CrossRef](#)]
20. Kirpich, I.A.; Gobejishvili, L.N.; Bon Homme, M.; Waigel, S.; Cave, M.; Arteel, G.; Barve, S.S.; McClain, C.J.; Deaciuc, I.V. Integrated hepatic transcriptome and proteome analysis of mice with high-fat diet-induced nonalcoholic fatty liver disease. *J. Nutr. Biochem.* **2011**, *22*, 38–45. [[CrossRef](#)]
21. Livak, K.J.; Schmittgen, T.D. Analysis of relative gene expression data using real-time quantitative PCR and the 2(-Delta Delta C(T)) Method. *Methods* **2001**, *25*, 402–408. [[CrossRef](#)]
22. Warner, J.; Hardesty, J.; Song, Y.; Sun, R.; Deng, Z.; Xu, R.; Yin, X.; Zhang, X.; McClain, C.; Warner, D.; et al. Fat-1 Transgenic Mice with Augmented n3-Polyunsaturated Fatty Acids Are Protected from Liver Injury Caused by Acute-On-Chronic Ethanol Administration. *Front. Pharmacol.* **2021**, *12*, 711590. [[CrossRef](#)]
23. Bailey, J.D.; Shaw, A.; McNeill, E.; Nicol, T.; Diotallevi, M.; Chuaiphichai, S.; Patel, J.; Hale, A.; Channon, K.M.; Crabtree, M.J. Isolation and culture of murine bone marrow-derived macrophages for nitric oxide and redox biology. *Nitric Oxide* **2020**, *100–101*, 17–29. [[CrossRef](#)] [[PubMed](#)]
24. Allenbach, C.; Zufferey, C.; Perez, C.; Launois, P.; Mueller, C.; Tacchini-Cottier, F. Macrophages induce neutrophil apoptosis through membrane TNF, a process amplified by *Leishmania major*. *J. Immunol.* **2006**, *176*, 6656–6664. [[CrossRef](#)] [[PubMed](#)]
25. Triantafyllou, E.; Woollard, K.J.; McPhail, M.J.W.; Antoniadou, C.G.; Possamai, L.A. The Role of Monocytes and Macrophages in Acute and Acute-on-Chronic Liver Failure. *Front. Immunol.* **2018**, *9*, 2948. [[CrossRef](#)]
26. Calvente, C.J.; Tameda, M.; Johnson, C.D.; Del Pilar, H.; Lin, Y.C.; Adronikou, N.; De Mollerat Du Jeu, X.; Llorente, C.; Boyer, J.; Feldstein, A.E. Neutrophils contribute to spontaneous resolution of liver inflammation and fibrosis via microRNA-223. *J. Clin. Investig.* **2019**, *129*, 4091–4109. [[CrossRef](#)]
27. Triantafyllou, E.; Pop, O.T.; Possamai, L.A.; Wilhelm, A.; Liaskou, E.; Singanayagam, A.; Bernsmeier, C.; Khamri, W.; Petts, G.; Dargue, R.; et al. MerTK expressing hepatic macrophages promote the resolution of inflammation in acute liver failure. *Gut* **2018**, *67*, 333–347. [[CrossRef](#)] [[PubMed](#)]
28. Marim, F.M.; Silveira, T.N.; Lima, D.S., Jr.; Zamboni, D.S. A method for generation of bone marrow-derived macrophages from cryopreserved mouse bone marrow cells. *PLoS ONE* **2010**, *5*, e15263. [[CrossRef](#)]
29. Yang, W.; Tao, Y.; Wu, Y.; Zhao, X.; Ye, W.; Zhao, D.; Fu, L.; Tian, C.; Yang, J.; He, F.; et al. Neutrophils promote the development of reparative macrophages mediated by ROS to orchestrate liver repair. *Nat. Commun.* **2019**, *10*, 1076. [[CrossRef](#)]
30. Mookerjee, R.P.; Stadlbauer, V.; Lidder, S.; Wright, G.A.; Hodges, S.J.; Davies, N.A.; Jalan, R. Neutrophil dysfunction in alcoholic hepatitis superimposed on cirrhosis is reversible and predicts the outcome. *Hepatology* **2007**, *46*, 831–840. [[CrossRef](#)]
31. Choi, H.K.; Kim, T.H.; Jhon, G.J.; Lee, S.Y. Reactive oxygen species regulate M-CSF-induced monocyte/macrophage proliferation through SHP1 oxidation. *Cell. Signal.* **2011**, *23*, 1633–1639. [[CrossRef](#)] [[PubMed](#)]
32. Karlsson, M.; Zhang, C.; Méar, L.; Zhong, W.; Digre, A.; Katona, B.; Sjöstedt, E.; Butler, L.; Odeberg, J.; Dusart, P.; et al. A single-cell type transcriptomics map of human tissues. *Sci. Adv.* **2021**, *7*, eabh2169. [[CrossRef](#)]
33. Williams, M.; Bonnardel, J.; Haest, B.; Vanderborght, B.; Wagner, C.; Remmerie, A.; Bujko, A.; Martens, L.; Thoné, T.; Browaeys, R.; et al. Spatial proteogenomics reveals distinct and evolutionarily conserved hepatic macrophage niches. *Cell* **2022**, *185*, 379–396.e38. [[CrossRef](#)]
34. He, H.Q.; Ye, R.D. The Formyl Peptide Receptors: Diversity of Ligands and Mechanism for Recognition. *Molecules* **2017**, *22*, 455. [[CrossRef](#)] [[PubMed](#)]
35. Dubuquoy, L.; Louvet, A.; Lassailly, G.; Truant, S.; Boleslawski, E.; Artru, F.; Maggioro, F.; Gantier, E.; Buob, D.; Leteurtre, E.; et al. Progenitor cell expansion and impaired hepatocyte regeneration in explanted livers from alcoholic hepatitis. *Gut* **2015**, *64*, 1949–1960. [[CrossRef](#)]
36. Owumi, S.E.; Corthals, S.M.; Uwaifo, A.O.; Kamendulis, L.M.; Klaunig, J.E. Depletion of Kupffer cells modulates ethanol-induced hepatocyte DNA synthesis in C57Bl/6 mice. *Environ. Toxicol.* **2014**, *29*, 867–875. [[CrossRef](#)] [[PubMed](#)]
37. García, R.A.; Lupisella, J.A.; Ito, B.R.; Hsu, M.Y.; Fernando, G.; Carson, N.L.; Allocco, J.J.; Ryan, C.S.; Zhang, R.; Wang, Z.; et al. Selective FPR2 Agonism Promotes a Proresolution Macrophage Phenotype and Improves Cardiac Structure-Function Post Myocardial Infarction. *JACC Basic Transl. Sci.* **2021**, *6*, 676–689. [[CrossRef](#)] [[PubMed](#)]
38. Dal-Secco, D.; Wang, J.; Zeng, Z.; Kolaczowska, E.; Wong, C.H.; Petri, B.; Ransohoff, R.M.; Charo, I.F.; Jenne, C.N.; Kubes, P. A dynamic spectrum of monocytes arising from the in situ reprogramming of CCR2+ monocytes at a site of sterile injury. *J. Exp. Med.* **2015**, *212*, 447–456. [[CrossRef](#)] [[PubMed](#)]
39. Caso, V.M.; Manzo, V.; Pecchillo Cimmino, T.; Conti, V.; Caso, P.; Esposito, G.; Russo, V.; Filippelli, A.; Ammendola, R.; Cattaneo, F. Regulation of Inflammation and Oxidative Stress by Formyl Peptide Receptors in Cardiovascular Disease Progression. *Life* **2021**, *11*, 243. [[CrossRef](#)] [[PubMed](#)]
40. Iimuro, Y.; Frankenberg, M.V.; Arteel, G.E.; Bradford, B.U.; Wall, C.A.; Thurman, R.G. Female rats exhibit greater susceptibility to early alcohol-induced liver injury than males. *Am. J. Physiol.* **1997**, *272 Pt 1*, G1186–G1194. [[CrossRef](#)]

41. Osna, N.A.; Donohue, T.M., Jr.; Kharbanda, K.K. Alcoholic Liver Disease: Pathogenesis and Current Management. *Alcohol Res.* **2017**, *38*, 147–161. [[PubMed](#)]
42. Robinson, M.W.; Harmon, C.; O'Farrelly, C. Liver immunology and its role in inflammation and homeostasis. *Cell. Mol. Immunol.* **2016**, *13*, 267–276. [[CrossRef](#)] [[PubMed](#)]

Disclaimer/Publisher's Note: The statements, opinions and data contained in all publications are solely those of the individual author(s) and contributor(s) and not of MDPI and/or the editor(s). MDPI and/or the editor(s) disclaim responsibility for any injury to people or property resulting from any ideas, methods, instructions or products referred to in the content.